2003

Production of fine Nd-Fe-B alloy powder by pulsed plasma atomization

Jeffrey E. Shield
University of Nebraska-Lincoln, jshield@unl.edu

S. Christensen
University of Utah

R. W. Kincaid
UTRON, Inc., Manassas, VA

F. D. Witherspoon
UTRON, Inc., Manassas, VA

Published in *Journal of Materials Science* 38 (2003), pp. 445–449.

Production of fine Nd-Fe-B alloy powder by pulsed plasma atomization

J. E. Shield
Department of Mechanical Engineering, University of Nebraska–Lincoln, Lincoln, NE 68588, USA
(Corresponding author, email jshield2@unl.edu)

S. Christensen
Department of Materials Science and Engineering, University of Utah, Salt Lake City, UT, USA

R. W. Kincaid, F. D. Witherspoon
UTRON, Inc., Manassas, VA, USA

Abstract

Extremely fine (<10 μm) Nd-Fe-B powder was generated by pulsed plasma atomization processing. The number average was just over 3 μm, as determined by computer-assisted scanning electron microscopy analysis of almost 3000 particles. Despite the fine particle size, alloys of stoichiometric $Nd_2Fe_{14}B$ resulted in the properitectic formation of α-Fe, deleteriously affecting the magnetic properties. Nevertheless, this work shows the possibility of generating extremely fine, isotropic powder for bonded and hybrid magnet applications.

1. Introduction

Rare earth permanent magnets, notably Nd-Fe-B, continue to grow in importance in commercial applications. In particular, bonded and hybrid magnet applications are rapidly expanding. These magnets require Nd-Fe-B powder with excellent isotropic properties. Commonly, the powder is produced by comminuting ribbon or flake produced by melt spinning. Directly producing powder of the desired size range with better morphological characteristics for injection molding (i.e., spherical powder) would lower magnet costs by easing processing. Inert gas atomization has been used to effectively produce Nd-Fe-B alloy powder with mean sizes on the order of tens of microns [1–3]. However, generally the solidification conditions are not severe enough, resulting in coarse microstructures and magnetic properties generally inferior to melt-spun material. Proper alloying has resulted in increased quenchability, leading to the formation of glassy material by atomization [4, 5]. However, conventional atomization processes result in coarser-than-desired powder for applications in hybrid and bonded magnets.

Alternate atomization techniques can result in the production of finer mean particle sizes. For example, pulsed plasma atomization has effectively produced Al and Cu powder in the sub-micron range [6]. In pulsed plasma atomization, the gas stream used in conventional gas atomization is replaced by short duration, high pressure pulses of plasma. The momentum flux provided by the plasma is significantly higher, sometimes three orders of magnitude, than even high pressure gas atomization processes. The higher momentum flux leads to more effective disintegration of the fluid streams, resulting in finer particles. In this paper, we explore the possibility of producing ultrafine Nd-Fe-B magnet powder by pulsed plasma atomization.

2. Experimental procedures

Alloys were prepared by arc-melting high-purity elemental Nd (99.9), Fe (99.9), and B (99.5) in an inert atmosphere with a stoichiometric $Nd_2Fe_{14}B$ composition. After several remelts to ensure homogeneity, the ingots were drop-cast into 0.375 in. diameter rods.* The rods were subsequently sectioned to produce cylinders approximately one inch in length.

These cylindrical rods were then used as consumable electrodes in a wire arc process. This wire arc process differed from conventional wire arc spray processes in two important ways. First, the continuous compressed gas that strips the molten droplets off the wire tips in conventional wire arc spraying was replaced with a pulsed plasma jet. This pulsed plasma jet operated at repetition rates as high as 60 Hz with pulse widths as long as 200 μs. The second significant divergence from wire arc spraying was that the arc between the wires was also a pulsed arc, and operated at the same repetition rate as the plasma jet. In this way, there was only molten material available at the wire tips when there was a plasma jet flowing past the wire tips. Additionally, the process used here utilized stationary rods as electrodes in contrast to moving wires. This was done for the sake of simplicity during the proof-of-concept phase.

* Arc melting and drop casting were provided by the Materials Preparation Center at Ames Laboratory, USDOE.

Both the arc between the electrodes and the plasma jet pulse are generated through the use of capacitor banks. These capacitor banks store energy until a trigger is initiated, at which time one capacitor bank dumps its energy through the capillary, forming the plasma, and the other capacitor bank dumps its energy into an arc formed between the two Nd-Fe-B rods. The pulsed arc heats and melts the surface of the Nd-Fe-B electrodes, and the pulsed plasma jet then strips and atomizes this molten material. This approach is an adaptation of a high velocity wire-arc spray device developed under a NASA Phase II SBIR program [7].

Powder collection was accomplished in several ways. First, an Al stub commonly used for mounting SEM samples was placed below the wire arc assembly. Atomized powder adhered to the double-stick carbon tape on the stub. This was effective in collecting SEM-ready powder, but not for collecting free powder for characterization by other techniques (e.g., x-ray diffraction). Subsequently, an open-mouthed collection bottle replaced the SEM stub. Up to a gram of material was effectively collected in this way. Finally, powder was collected off of the walls of the chamber with double- stick carbon tape. This latter technique tended to gather the finest powder and was not representative of the overall powder size. Nevertheless, it provided information on the finest size powder produced.

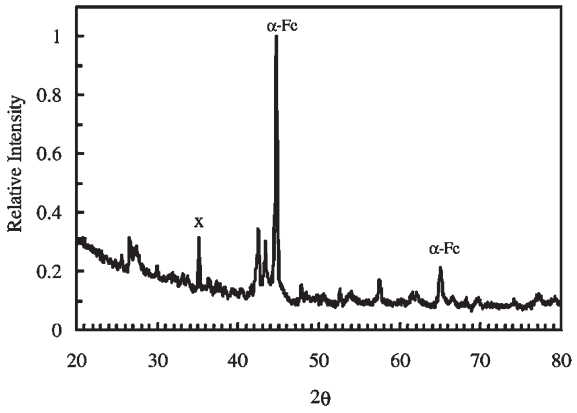

Figure 1. X-ray diffraction pattern of the –100 μm sieved powder. The α-Fe peaks are marked, as is the unknown phase (with an "X"). All other peaks correspond to the $Nd_2Fe_{14}B$ structure.

Powder was examined by scanning electron microscopy utilizing a Hitachi S-3000N. As-atomized powder and sectioned specimens was examined. Energy dispersive x-ray spectroscopy (EDS) was used to obtain powder chemistry. This was primarily done on larger particles after polishing in order to obtain more reliable results. The EDS spectra were analyzed by standardless techniques using an EDAX Phoenix system to obtain chemical compositions.

The powder was classified by initially coarse sieving at 100 μm to eliminate splats and larger "shrapnel" type material that could misrepresent powder properties. The –100 μm classification was examined thoroughly. A detailed size classification of the –100 μm powder was accomplished with computer-controlled scanning electron microscopy utilizing EDAX particle analysis software. With this technique, images were captured and then the software automatically identified powder characteristics, including size and sphericity. Care was taken to avoid high powder density, which would lead to particle overlap and ambiguous particle determination. The ability of the software to discern very fine particles was also checked by manual examination. It was found that the software did an excellent job of finding particles down to approximately 100 nm.

The powder examined by x-ray diffraction for phase analysis utilizing a Philips MPD powder diffractometer with

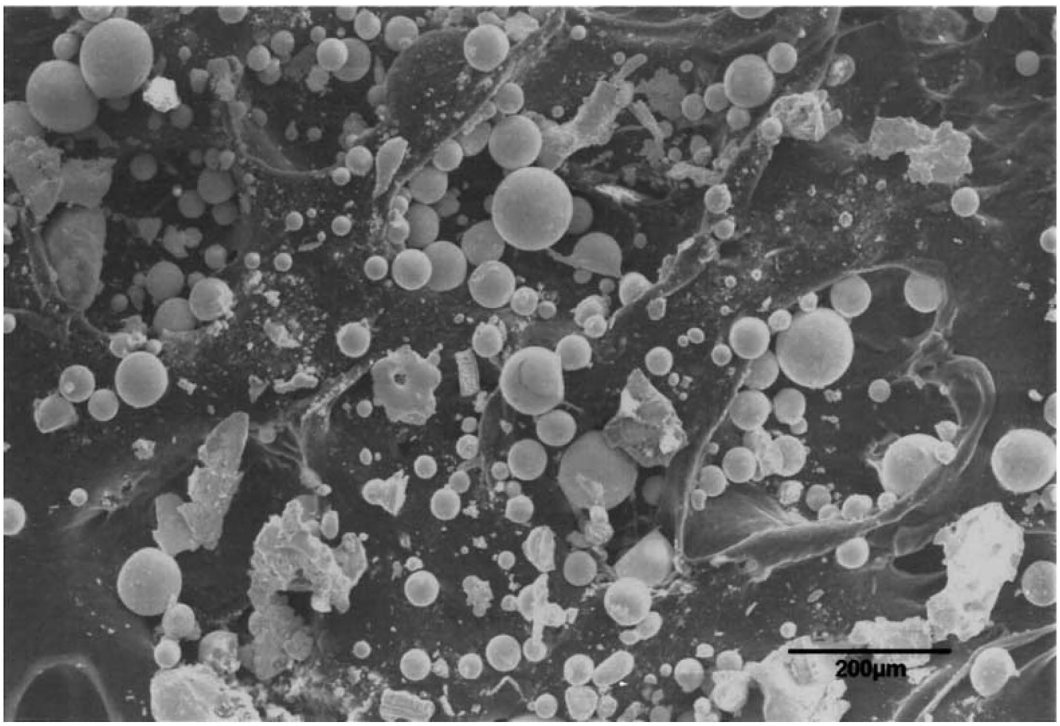

Figure 2. Scanning electron micrograph of the –100 μm sieved powder.

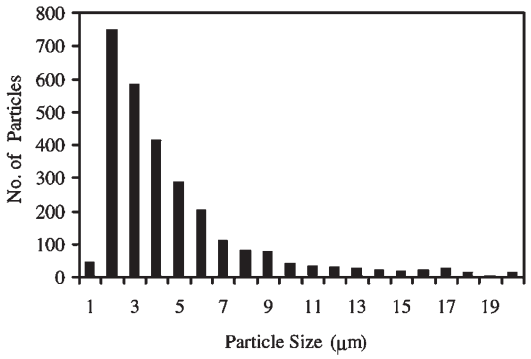

Figure 3. Number distribution of particles in the –100 μm sieved powder section, as determined from computer-controlled SEM analysis.

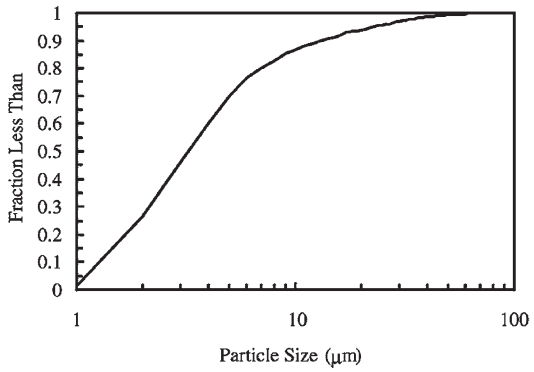

Figure 4. Cumulative number fraction finer as a function of particle size for the –100 μm sieved powder. The mean particle diameter was determined to be 3.5μm.

Cu K_α x-rays. The powder was mounted on an offcut SiO_2 single crystal to effectively eliminate background. The magnetic properties were measured on powder mounted in wax using a Lakeshore vibrating sample magnetometer at ambient temperature.

3. Results and discussion

Powder of $Nd_2Fe_{14}B$ was produced and collected in sufficient quantity for relatively thorough characterization. Powder was initially sieved into two classifications: +100 μm and –100 μm. The phase constituency of the +100 μm cut consisted of $Nd_2Fe_{14}B$, α-Fe, and a Nd-rich phase, as determined by x-ray diffraction and SEM analysis. The phase constituency of the –100 μm cut consisted primarily of $Nd_2Fe_{14}B$ and α-Fe, as shown in Figure 1. A diffraction peak at approximately 35° 2θ was not able to be indexed. It likely is due to the presence of a Nd-rich phase. No evidence of amorphous phase formation was observed. Additionally, numerous "splats" were observed in the +100 μm classification, indicating that some powder was molten when colliding with chamber walls, etc. The presence of α-Fe in the –100 μm cut indicated that cooling rates were not sufficient to bypass the formation of α-Fe during solidification. Normally, the presence of α-Fe leads to a reduction in magnetic performance by enabling the demagnetization process.

Scanning electron microscopy of the –100 μm cut revealed spherical powder in a range of sizes (Figure 2). Typical powder sizes ranged from a few tenths of a micron to tens of microns. The observed powder also was very spherical, as seen

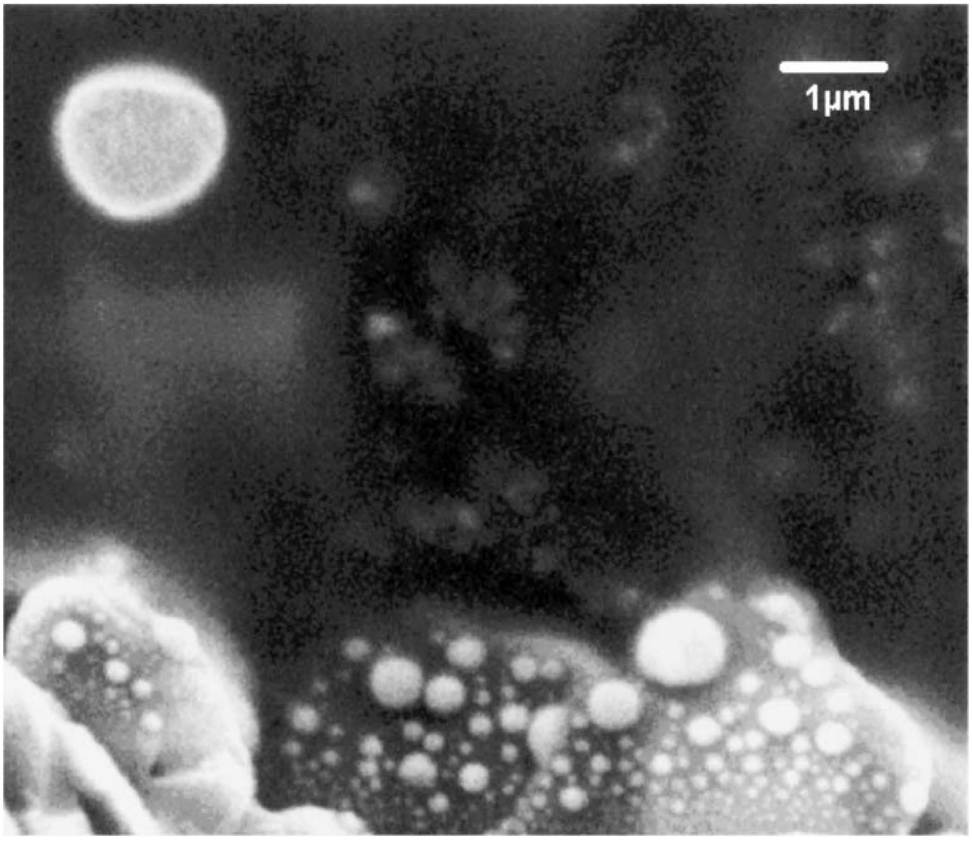

Figure 5. Scanning electron micrographs of the finer powder sizes observed.

in Figure 2, and lacked satellite particles even on larger particles. The average size of the powder examined, utilizing computer-controlled SEM and analysis, was approximately 6.5 μm. The number distribution of the particles is shown in Figure 3. A single maximum was observed, and the number distribution is extremely narrow with very few particles greater than 10 μm. The cumulative number fraction finer than a given particle size is shown in Figure 4. The mean diameter, given at a fraction finer than 0.5, is approximately 3.5 μm. Approximately 90 percent of the particles were finer than approximately 10.5 μm. It should be noted that very fine powder was difficult to quantify at the magnification at which this analysis was conducted, thereby leading to an undercounting of very fine powder. Figure 5 shows SEM micrographs of extremely fine particles collected from chamber walls. Powder on the order of 100 nm was routinely observed.

The classified powder was mounted and polished, and the internal microstructure examined by SEM. Backscattered electron images of two particles are shown in Figure 6. Typically, the powder in the –100 μm classification displayed a two-phase microstructure; although larger particles (>30 μm) contained a third, Nd-rich phase. The absence of a third, Nd-

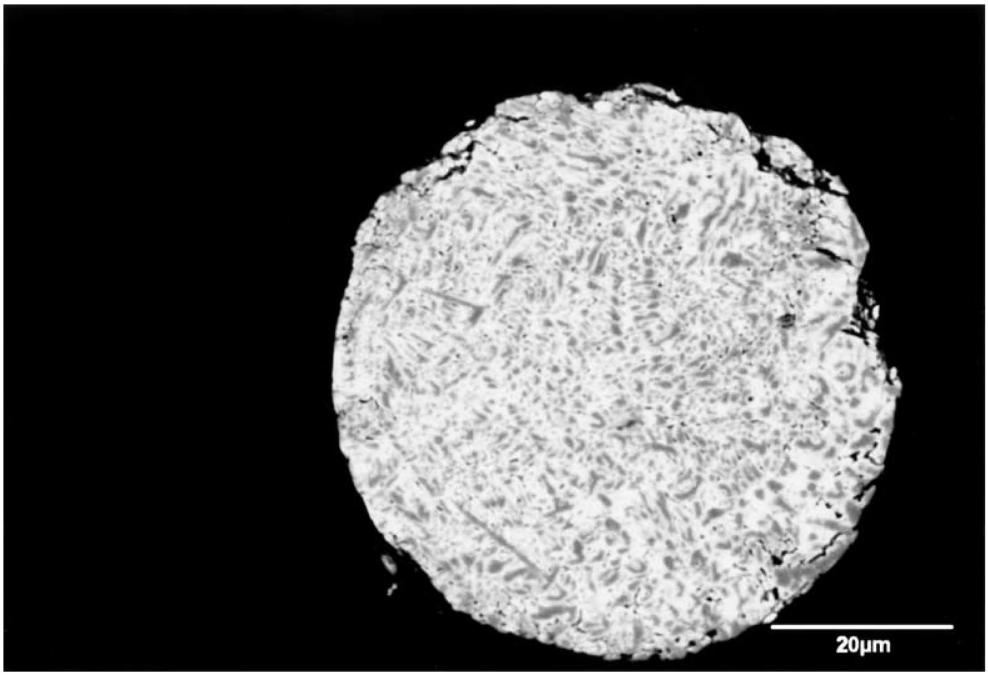

(a)

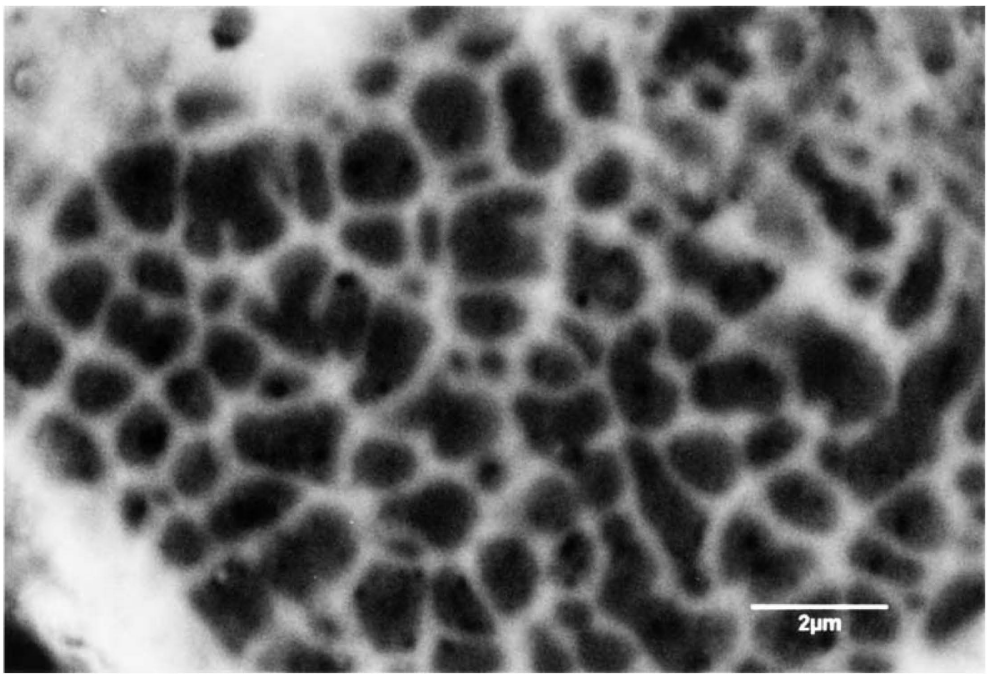

Figure 6. Backscattered electron micrographs showing the internal microstructure of –100 μm sieved powder. The two micrographs are of different particles.

rich phase in the finer particles, as required by a mass balance, is thought to be from a lack of detectability. The finer particles have a higher undercooling, thereby reducing the amount of primary Fe formation and subsequent amount of the third, balancing phase, rendering it difficult to observe. The microstructure generally consisted of relatively equiaxed α-Fe grains surrounded by the $Nd_2Fe_{14}B$ phase. Clearly dendritic α-Fe was observed in some cases. The observed microstructure is typical of peritectic solidification, with primary, properitectic formation of α-Fe followed by peritectic formation of $Nd_2Fe_{14}B$. The existence of α-Fe as the primary solidification product indicates that the undercooling was not sufficient to bypass the formation of α-Fe. The undercooling is associated with cooling rate, so that higher cooling rates are necessary for proper phase formation. Compositional analysis utilizing energy dispersive x-ray spectroscopy (EDS) revealed the correct stoichiometry, indicating that near-nominal compositions were maintained.

The presence of α-Fe at this scale deleteriously affects the magnetic properties. The hysteresis loop of the –100 μm powder reveals low coercivity (270 Oe) and remanence (Figure 7). The coarse $Nd_2Fe_{14}B$ grains are in a multidomain state, resulting in soft magnetic behavior, and the α-Fe further eases the magnetization reversal. The smooth loop shape reflects a lack of any powder in the sample, even very fine particles, with a desirable microstructure. Any powder fraction with an appropriate microstructure would result in a distorted loop shape and a higher coercivity. Therefore, indications are that even the finest size ranges lack appropriate microstructures for hard magnetic applications. However, microstructural evolution, including phase formation and scale, likely can be further controlled through proper alloy development.

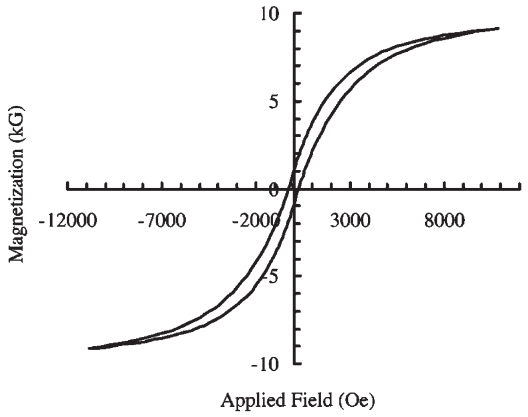

Figure 7. Magnetization versus applied magnetic field behavior for the –100 μm sieved powder.

4. Conclusions

Fine, spherical Nd-Fe-B magnet powder was produced by pulsed plasma atomization with a mean diameter of 6 μm, and a number average of approximately 2 μm. The composition of the atomized powder was nominally the same as the starting composition, and no contamination was observed. However, solidification involved the formation of primary Fe, with deleterious affects on the magnetic properties. The coercivity was observed to be only 270 Oe, with no indication of very fine powder having appropriately fine microstructures. Clearly, the cooling rate in pulsed plasma atomization is not sufficiently high to generate desirable microstructures in the Nd-Fe-B system. Further studies will include controlling the phase evolution and microstructural scale by altering the composition and through alloying additions, with the result being significant improvement in magnetic properties. Optimization of this technique will lead to applications of the atomized Nd-Fe-B powder in hybrid and bonded magnets.

Acknowledgments

The authors are grateful for assistance with the magnetic measurements from S. Guruswamy and N. Srisukhumbowornchai of the University of Utah, and for funding from the National Science Foundation through Grant No. DMI0060764.

References

1. M. Yamamoto, A. Inoue, and T. Masumoto, *Met. Trans. A* 20A (1989) 5.
2. C. M. Hsu, H. M. Lin, R. W. Mccallum, I. E. Anderson, and B. K. Lograsso, *Mat. Chem. Phys.* 42 (1995) 148.
3. C. H. Sellers, T. A. Hyde, D. J. Branagan, L. H. Lewis, and V. Panchanathan, *J. Appl. Phys.* 81 (1997) 1351.
4. D. J. Branagan, T. A. Hyde, C. H. Sellers and R. W. McCallum, *J. Phys. D* 29 (1996) 2376.
5. D. J. Branagan, T. A. Hyde, C. H. Sellers, and L. H. Lewis, *IEEE Trans. Magn.* 32 (1996) 5097.
6. F. D. Witherspoon, *Powder Metallurgy* 43 (2000) 318.
7. R. W. Kincaid and F. D. Witherspoon, in Proceedings of the International Thermal Spray Conference 2000, Montreal, Canada, May 8–11, 2000.

Submitted 29 March 29, 2002, accepted September 9, 2002.